Back to Einstein: how to include burial in fluvial sediment diffusion models?

James K. Pierce [1] and **Marwan A. Hassan**[1]

[1]Department of Geography

University of British Columbia

Key Points:

- We develop a random walk model of objects in intermittent transport through an environment with traps
- Its solution provides three ranges of diffusion, two of which are anomalous
- We apply the model to sediment transport in rivers to clarify the scale dependence of bedload diffusion

Corresponding author: James Kevin Pierce, `kpierce@alumni.ubc.ca`

Abstract

Sediment grains transport through gravel bed rivers in cycles of motion and rest. When grains rest on the surface, material transported from upstream can bury them. The surface shields buried grains from the flow, so they can be immobile for long time periods. These immobile periods can dominate sediment diffusion characteristics. Although investigators have recognized the impact of sediment burial on diffusion, existing models do not usually incorporate it. In this study, we present a random walk model incorporating sediment burial and solve it analytically. The model predicts three sediment diffusion ranges with distinct scaling characteristics in each. We relate the crossover times dividing these ranges to measurable transport parameters and describe each range from underlying physical processes. Our developments provide new geophysical perspective on the scale dependence of fluvial sediment transport.

1 Introduction

Anomalous diffusion has been subjected to intense research lately, as it emerges in contexts ranging from the transport of cholesterols through lipid bilayers (Jeon, Monne, Javanainen, & Metzler, 2012; Molina-Garcia et al., 2018), to contaminants through soils (Berkowitz, Cortis, Dentz, & Scher, 2006; X. R. Yang & Wang, 2019), and pollinator insects through ecosystems (Reynolds & Rhodes, 2009; Vallaeys, Tyson, Lane, Deleersnijder, & Hanert, 2017). In this paper, we study anomalous diffusion in a river science context, where it emerges from coarse bedload sediment transporting through river channels (N. D. Bradley, 2017; Ganti, Meerschaert, Foufoula-Georgiou, Viparelli, & Parker, 2010; Martin, Jerolmack, & Schumer, 2012). Hans Albert Einstein developed the first model of bedload diffusion to describe his comprehensive experiments visually tracking painted grains through a flume (H. A. Einstein, 1937; Ettema & Mutel, 2004). Diffusion is the spreading apart of grains as they transport downstream, and it is induced by differences in the transport characteristics of one grain and the next. Diffusion is usually quantified by the time dependence of the positional variance $\sigma_x^2(t)$ of a population. With the scaling $\sigma_x^2 \propto t$, the diffusion is said to be normal, since this is found in the classic diffusion problems (e.g., A. Einstein, 1905; Taylor, 1920). However, many transport phenomena show $\sigma_x^2 \propto t^\gamma$ with $\gamma \neq 1$. This diffusion is said to be anomalous (Sokolov, 2012). If $\gamma > 1$, it is said to be super-diffusive; while if $\gamma < 1$, it is said to be sub-diffusive

(Metzler & Klafter, 2000). Einstein originally concluded that bedload transport shows normal diffusion.

After Einstein, Nikora, Habersack, Huber, and McEwan (2002); Nikora, Heald, Goring, and McEwan (2001) recognized that coarse sediment moving through river channels can show either anomalous or normal diffusion depending on the timescale of observation. This is a significant issue since it implies diffusion models should be scale dependent, and it renders experimental data contingent on their observation timescales. Nikora et al. identified three ranges of diffusion from Newtonian simulations and experimental data and termed these ranges local, intermediate, and global in order of increasing timescale. They determined that σ_x^2 scales with a different power of time in each range, and they concluded this scaling could be anomalous or normal. Recent studies support the Nikora et al. conclusion that bedload diffusion is scale dependent, but they do not show consensus on the details of their three range concept. For example, various numerical approaches show two (e.g., Fan, Singh, Guala, Foufoula-Georgiou, & Wu, 2016) or three (e.g., Bialik, Nikora, & Rowiński, 2012; Zhang, Meerschaert, & Packman, 2012) ranges of diffusion; one set of flume experiments shows two ranges of sediment diffusion (Martin et al., 2012), and two field studies show anomalous diffusion (N. D. Bradley, 2017; Phillips, Martin, & Jerolmack, 2013); but taken together, these studies leave us unclear on the expected number of diffusion ranges and the scaling (super/normal/sub) of each range. Up to now, no model has been developed to derive three diffusion ranges from process based concepts of fluvial sediment transport.

In this study, we develop a model of bedload diffusion that describes the local, intermediate, and global ranges of diffusion introduced by Nikora et al. by generalizing the original diffusion model of H. A. Einstein (1937). Einstein was a giant in river geophysics and fostered an entire paradigm of research leveraging and generalizing his stochastic methods (e.g., Gordon, Carmichael, & Isackson, 1972; Hubbell & Sayre, 1964; Nakagawa & Tsujimoto, 1976; C. T. Yang & Sayre, 1971; Yano, 1969). His original model's essential content is that individual grains move in instantaneous steps interrupted by durations of rest which lie on statistical distributions (Hassan, Church, & Schick, 1991). Einstein's model can be viewed as a special case of the continuous time random walk (CTRW) developed by Montroll and Weiss (1965) in condensed matter physics to describe the diffusion of charge carriers in solids. Our generalization of Einstein's model has two components. First, we include the duration and velocity of motions in place of instantaneous

76   steps, and second, we add in the process of sediment burial, which has been associated

77   with anomalous diffusion at long timescales (e.g., N. D. Bradley, 2017; Martin, Puro-

78   hit, & Jerolmack, 2014). To develop this generalization, we leverage the multi state CTRW

79   developed by Weiss (1976, 1994) that extends the CTRW of Montroll and Weiss (1965).

80   Below, we develop the model in section 2 and solve it in section 3. Finally, we discuss

81   the predictions of our model and its implications for scale dependent bedload transport

82   in sections 4 and 5.

2 Bedload diffusion with burial as a multi state random walk

84   Following Einstein, we describe bedload transport as a random walk between mo-

85   bile and immobile states. However, we carefully distinguish two states of immobility: grains

86   can be immobile on the surface, which we refer to as the "resting state", or grains can

87   be immobile within the sub-surface, which we refer to as the "burial state". To model

88   bedload transport with both of these immobile states, we construct a three-state ran-

89   dom walk where the states are motion, rest, and burial, and we label these states as $i =$

90   2 (motion), $i = 1$ (rest), and $i = 0$ (burial). Our development of the governing equa-

91   tions for the three state walk follows Weiss (1994), and our incorporation of the sediment

92   burial process is similar to Schmidt, Sagués, and Sokolov (2007). In our model, times

93   spent moving or resting on the bed surface are random variables characterized by ex-

94   ponential distributions, and moving grains have a constant velocity v. Within the model,

95   we consider burial to be a relatively long lasting condition that has some probability to

96   occur when grains resting on the surface are covered by transported sediment. The prob-

97   ability of burial per unit time (burial rate) is considered constant, so the probability that

98   grains become buried increases with the time they rest.

99   Our derivation hinges on the concept of a sojourn in the state i (Weiss, 1994). When

100   a grain enters a state i at some time t_0 and position x_0, then leaves a state at some other

101   time t_1 and position x_1, we say that the grain has completed a sojourn in the state i.

102   The joint probability density for a complete sojourn in the state i of time $t = t_1 - t_0$

103   and displacement $x = x_1 - x_0$ is denoted $g_i(x, t)$. Similarly, we consider incomplete so-

104   journs. If a grain begins a sojourn in the state i at (t_0, x_0) and the sojourn is still on-

105   going at (x_1, t_1), the joint probability density to find the grain is $G_i(x, t)$. We refer to

106   g_i and G_i as the complete and incomplete propagators, since they move probability through

107   space-time and are associated respectively with complete and incomplete sojourns.

108   Our target is the probability distribution $p(x, t)$ to find a grain at x, t if we know

109   it started at $(x, t) = (0, 0)$; that is, if it started with the initial distribution $p(x, 0) =$

110    $\delta(x)$. We denote the initial probabilities to be at rest or in motion as θ_1 and θ_2. Nor-

111   malization requires $\theta_1 + \theta_2 = 1$. Our derivation has two main stages. First, we intro-

112   duce and solve for a set of joint probabilities associated with transitions of a grain from

113   one state to another. Second, we use these quantities to solve for the probabilities that

114   a grain is in state i having position x at time t. Afterward, we sum these latter distri-

115   butions over all states i to derive the joint distribution that a grain is in any state at (x, t).

116   Now we begin the first stage of the derivation. Grains at rest may be trapped by

117   burial. For simplicity, we model burial as long lasting enough to be effectively perma-

118   nent (e.g., Wu et al., 2019), and we assume grains resting on the surface can be buried

119   with constant rate κ. Equivalently, we could say the mean time required for a resting

120   grain to become buried is $1/\kappa$. From this assumption, the probability that a grain is not

121   trapped after a time t at rest obeys a survival function: $\Phi_F(t) = e^{-\kappa t}$ (F is for "free").

122   Likewise, the probability that it is trapped after resting for a time t is the complement:

123    $\Phi_T(t) = 1 - \Phi_F(t)$ (T is for "trapped"). We introduce $\omega_{1T}(x, t)$, $\omega_{1F}(x, t)$, and $\omega_2(x, t)$

124   as the joint probabilities to find a grain at (x, t) having just completed a sojourn. The

125   subscript $1T$ denotes the completion of a rest sojourn due to trapping by burial, while

126    $1F$ denotes the completion of a rest sojourn due to motion. Similarly, the subscript 2

127   denotes the completion of a motion sojourn due to resting. We link the ω's in integral

128   equations using an argument similar to Weiss (1994):

$$\omega_{1T}(x, t) = \theta_1 \Phi_T(t) g_1(x, t) + \int_0^x dx' \int_0^t dt' \omega_2(x', t') \Phi_T(t - t') g_1(x - x', t - t'), \quad (1)$$

$$\omega_{1F}(x, t) = \theta_1 \Phi_F(t) g_1(x, t) + \int_0^x dx' \int_0^t dt' \omega_2(x', t') \Phi_F(t - t') g_1(x - x', t - t'), \quad (2)$$

$$\omega_2(x, t) = \theta_2 g_2(x, t) + \int_0^x dx' \int_0^t dt' \omega_{1F}(x', t') g_2(x - x', t - t'). \quad (3)$$

129   The first equation can be understood as follows: $\omega_{1T}(x, t)$ describes the probability that

130   a sojourn in the state 1 ends due to trapping at (x, t). This quantity has two contribu-

131   tions. The first contribution represents the possibility that the grain started at $(x, t) =$

132    $(0, 0)$ in the $i = 1$ state (with probability θ_1), propagated a distance x and a time t in

133   the $i = 1$ state (with probability density $g_1(x, t)$), was trapped (with probability $\Phi_T(t)$),

134   and is now at (x, t). The second contribution describes the possibility that the grain was

135   in a motion sojourn which ended at (x', t') when it came to rest. From here, it propa-

136   gated from (x', t') to (x, t) at rest (with probability density $g_1(x - x', t - t')$) and was

137   trapped during this sojourn (with probability $\Phi_T(t-t')$). The reasoning is closely anal-

138   ogous for equations (2) and (3). Once the propagators are specified, we can solve (1-3)

139   for the ω's to complete the first stage of the derivation.

140   The second stage of our derivation involves the joint probabilities of being in state

141   regardless of whether a sojourn has just completed. We denote these by $p_0(x,t)$ (trapped),

142    $p_1(x,t)$ (rest), and $p_2(x,t)$ (motion), and we involve the ω's in their definition:

$$p_0(x,t) = \int_0^t dt' \omega_{1T}(x, t-t'), \tag{4}$$

$$p_1(x,t) = \theta_1 G_1(x,t) + \int_0^x dx' \int_0^t dt' \omega_2(x',t') G_1(x-x', t-t'), \tag{5}$$

$$p_2(x,t) = \theta_2 G_2(x,t) + \int_0^x dx' \int_0^t dt' \omega_{1F}(x',t') G_2(x-x', t-t'). \tag{6}$$

143   Equation (4) says that grains buried at any (x,t) were trapped at x from any earlier times.

144   The reasoning in (5-6) is the same as for (1-3) except we use the propagators for incom-

145   plete sojourns. Equations (4-6) can be solved once the propagators are specified and the

146   ω's are derived from (1-3). Finally, we form the total probability density for a grain to

147   be found at (x,t) in any state. This is simply

$$p(x,t) = p_0(x,t) + p_1(x,t) + p_2(x,t). \tag{7}$$

148   This joint density was our target and is completely determined once (1-6) are solved.

3   Specification of propagators and solution of model

150   We consider sojourns in the rest state to occur for an exponentially distributed time

151   interval given by the distribution $\psi_1(t) = k_1 e^{-k_1 t}$. The probability that a sojourn in

152   this state lasts for at least a time t is then $\Psi_1(t) = \int_t^\infty \psi_1(t) dt = e^{-k_1 t}$. $1/k_1$ is the

153   mean duration of a single rest. Since grains do not move in the rest sojourn, the prob-

154   ability density that a grain is displaced by a distance x in the rest sojourn in $\delta(x)$. Hence

155   the complete propagator for rest sojourns is $g_1(x,t) = \delta(x)\psi_1(t)$, or

$$g_1(x,t) = \delta(x) k_1 e^{-k_1 t}. \tag{8}$$

156   Likewise, the incomplete propagator for a rest sojourn is $G_1(x,t) = \delta(x)\Psi_1(t) = \delta(x)e^{-k_1 t} =$

157    $g_1(x,t)/k_1$. The motion propagators are reasoned similarly. We consider motions to have

158   a constant velocity v and exponentially distributed durations given by $\psi_2(t) = k_2 e^{-k_2 t}$.

159    $1/k_2$ is the mean duration of a single motion. Since the velocity of motions is constant,

the probability to find a grain at position x in a motion sojourn is $\delta(x - vt)$, and the complete propagator for motion sojourns is

$$g_2(x, t) = \delta(x - vt)k_2 e^{-k_2 t}, \tag{9}$$

while the incomplete propagator is $G_2(x, t) = g_2(x, t)/k_2$ as before.

Having defined the propagators, we set out to solve (1-6) and understand the diffusion expressed by the trapping model. The convolution structure of equations (1-6) presents a formidable problem. Luckily, we have the device of Laplace transforms. These project integro-differential equations into an alternate space in which convolutions are unraveled (e.g., Arfken, 1985). The double Laplace transform of a joint probability distribution $p(x, t)$ is defined by

$$\tilde{p}(\eta, s) = \int_0^\infty dx e^{-\eta x} \int_0^\infty dt e^{-st} p(x, t). \tag{10}$$

The Laplace-transformed moments of x are linked to derivatives of the double transformed distribution (10) (cf., Berezhkovskii & Weiss, 2002). From equation (10) it's clear that

$$\langle \tilde{x}(s)^k \rangle = (-)^k \partial_\eta^k \tilde{p}(\eta, s) \Big|_{\eta=0}. \tag{11}$$

The operator $\langle \circ \rangle$ denotes the ensemble average (e.g., Kittel, 1958). This means we can compute the variance of position as $\sigma_x^2(t) = \langle x^2 \rangle - \langle x \rangle^2 = \mathcal{L}^{-1}\{\langle \tilde{x}^2 \rangle; t\} - \mathcal{L}^{-1}\{\langle \tilde{x} \rangle; t\}^2$, where $\mathcal{L}^{-1}$ denotes the inverse Laplace transform (e.g., Arfken, 1985). This is a powerful tool, since we can use it to derive the positional variance without integrating the distribution in equation (7).

Using the propagators (8-9) and this transform calculus, the joint distribution $p(x, t)$ is derived in appendix A, while the moments $\langle x \rangle$ and $\langle x^2 \rangle$ and ultimately the variance of position $\sigma_x^2(t)$ are derived in appendix B. With the shorthand notations $\xi = k_2 x/v$, $\tau = k_1(t - x/v)$, and $\Omega = (\kappa + k_1)/k_1$ (cf., Lisle et al., 1998), the joint distribution to find a grain at position x at time t is

$$
\begin{aligned}
p(x, t) = {} & \theta_1 \mathcal{H}(\xi)\mathcal{H}(\tau)\Big[1 - \frac{k_1}{\kappa + k_1}\Big(1 - e^{-(\kappa+k_1)t}\Big)\Big]\delta(x) \\
& + \frac{1}{v}e^{-\Omega\tau-\xi}\mathcal{H}(\xi)\mathcal{H}(\tau)\Big(\theta_1\Big[k_1\mathcal{I}_0\big(2\sqrt{\xi\tau}\big) + k_2\sqrt{\frac{\tau}{\xi}}\mathcal{I}_1\big(2\sqrt{\xi\tau}\big)\Big] \\
& \quad + \theta_2\Big[k_1\delta(\tau) + k_2\mathcal{I}_0\big(2\sqrt{\xi\tau}\big) + k_1\sqrt{\frac{\xi}{\tau}}\mathcal{I}_1\big(2\sqrt{\xi\tau}\big)\Big]\Big) \\
& + \frac{1}{v}\frac{\kappa k_2}{\kappa + k_1}e^{-\kappa\xi/(\kappa+k_1)}\mathcal{H}(\xi)\mathcal{H}(\tau)\Big[(\theta_1/\Omega)\mathcal{P}_2(\xi/\Omega, \Omega\tau) + \theta_2\mathcal{P}_1(\xi/\Omega, \Omega\tau)\Big]. \quad (12)
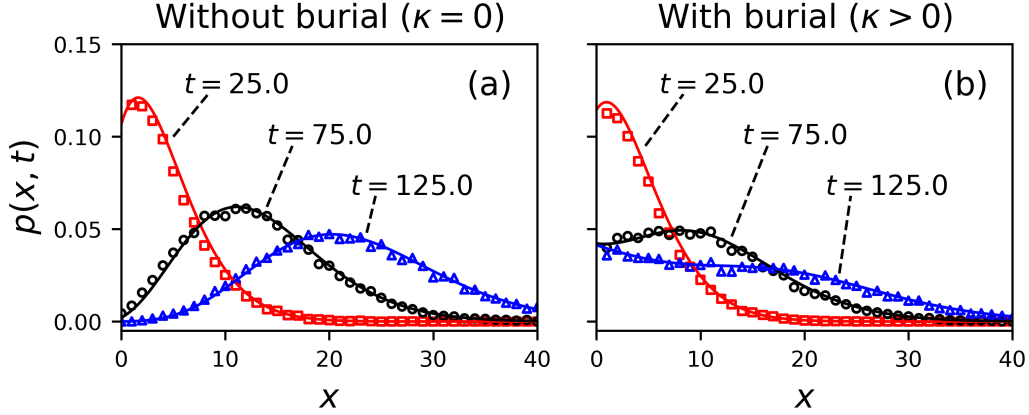\end{aligned}
$$

Figure 1. Joint distributions for a grain to be at position x at time t are displayed for the choice $k_1 = 0.1$, $k_2 = 1.0$, $v = 2.0$. Grains are considered initially at rest ($\theta_1 = 1$, $\theta_2 = 0$). The solid lines are the analytical distribution in equation (12), while the points are simulation results to show mathematical correctness. Colors pertain to different times. Units are unspecified, since our aim is to demonstrate the general characteristics of $p(x, t)$. Panel (a) shows the case $\kappa = 0$ – the absence of burial. In this case, the joint distribution tends toward Gaussian at large times (e.g., H. A. Einstein, 1937; Lisle et al., 1998). Panel (b) shows the case when grains have rate $\kappa = 0.01$ to become buried while resting. Because of burial, the joint distribution tends toward a more uniform distribution than Gaussian. This shows a redistribution of probability to smaller values of x due to the burial process (cf., Wu et al., 2019). The redistribution is encoded mathematically by the Marcum Q-function terms in equation (12). A similar tendency is seen in field studies of tracer dispersion in gravel bed rivers (e.g., Hassan & Church, 1994).

181    $\mathcal{H}$ is the Heaviside step function and we use the convention $\mathcal{H}(0) = 1$. The $\mathcal{I}_\nu$ are mod-

182   ified Bessel functions of the first kind, and the $\mathcal{P}_\mu$ are generalized Marcum Q-functions

183   defined by $\mathcal{P}_\mu(x, y) = \int_0^y e^{-z-x} (z/x)^{(\mu-1)/2} \mathcal{I}_{\mu-1}(2\sqrt{xz}) dz$ (Temme, 1996). Modified

184   Bessel functions are common in one-dimensional diffusion problems (e.g., Daly & Por-

185   porato, 2010; H. A. Einstein, 1937; Giddings & Eyring, 1955).

186   The Marcum Q-functions are convolutions between modified Bessel functions and

187   decaying exponentials. They were originally devised in relation to radar detection the-

188   ory (Marcum, 1960). Conceptually, the Q-functions emerge in our context from the sed-

189   iment burial process. According to our assumptions, resting grains can become buried

190   in some interval of time with an exponential probability. Meanwhile, the probability that

191 grains are resting follows a modified Bessel distribution (e.g., H. A. Einstein, 1937; Lisle

192 et al., 1998). As a result, the probability that sediment is resting and becomes buried

193 involves the convolution structure of the Marcum Q-functions. Consistent with this in-

194 terpretation, terms involving these convolutions vanish when the burial rate is taken to

195 zero ($\kappa \to 0$). Figure 1 depicts the distribution (12) alongside simulations generated

196 by a direct method based on evaluating the cumulative transition probabilities between

197 states on a small timestep (cf., Barik, Ghosh, & Ray, 2006). A link to the simulation code,

198 which includes descriptive comments, is available in the acknowledgments.

199 The first two moments and the positional variance are derived in appendix B. The

200 moments are

$$\langle x(t) \rangle = A_1 e^{(b-a)t} + B_1 e^{-(a+b)t} + C_1, \tag{13}$$

$$\langle x^2(t) \rangle = A_2(t) e^{(b-a)t} + B_2(t) e^{-(a+b)t} + C_2. \tag{14}$$

201 In these equations, $a = (\kappa + k_1 + k_2)/2$ and $b = \sqrt{a^2 - \kappa k_2}$ are effective rates having

202 dimensions of inverse time. The A_i, B_i, and C_i are polynomials available in table 1. The

203 variance is

$$\sigma_x^2(t) = A(t) e^{(b-a)t} + B(t) e^{-(a+b)t} + C(t). \tag{15}$$

204 A, B, and C are transcendental functions available in table 1. This equation represents

205 the scale dependence of bedload diffusion for sediment gradually undergoing burial.

206 The positional variance is plotted in figure 2 for conditions $\theta_1 = 1$ and $k_2 \gg k_1 \gg$

207 κ. We interpret "$\gg$" to mean "of at least an order of magnitude greater". These con-

208 ditions mean that all grains are initially at rest (cf., Wu et al., 2019), motion intervals

209 are typically much shorter than rests (cf., H. A. Einstein, 1937), and sediment burial re-

210 quires a much longer time than typical rests. We concentrate on these conditions in this

211 paper as they are most relevant to bedload diffusion in gravel-bed rivers, where sediment

212 transport is typically rarefied and intermittent, and the burial process is relatively slow

213 compared to surface resting times (e.g., Ferguson & Hoey, 2002; Hassan & Church, 1994).

214 Figure 2 demonstrates that under these conditions the variance (15) shows three ranges

215 of bedload diffusion each having approximate power law scaling ($\sigma_x^2 \propto t^\gamma$), followed by

216 a fourth range with no diffusion ($\sigma_x^2 = \text{const}$). We associate the first three ranges with

217 the local, intermediate, and global ranges proposed by Nikora et al. (2002, 2001), and

218 identify the fourth range as resulting from the eventual burial of all sediment grains. We

219 suggest to call the fourth range geomorphic, since any further transport in this range can

Table 1. Polynomials and transcendental functions used in the expressions of the mean (13), second moment (14) and variance (15) of bedload tracers.

$$A_1 = \frac{v}{2b}\Big[\theta_2 + \frac{k_1 + \theta_2\kappa}{b - a}\Big]$$

$$B_1 = -\frac{v}{2b}\Big[\theta_2 - \frac{k_1 + \theta_2\kappa}{a + b}\Big]$$

$$C_1 = -\frac{v}{2b}\Big[\frac{k_1 + \theta_2\kappa}{b - a} + \frac{k_1 + \theta_2\kappa}{a + b}\Big]$$

$$A_2(t) = \frac{v^2}{2b^3}\Big[(bt - 1)[k_1 + \theta_2(2\kappa + k_1 + b - a)] + \theta_2 b$$
$$+ \frac{(\kappa + k_1)(\theta_2\kappa + k_1)}{(b - a)^2}[(bt - 1)(b - a) - b]\Big]$$

$$B_2(t) = \frac{v^2}{2b^3}\Big[(bt + 1)[k_1 + \theta_2(2\kappa + k_1 - a - b)] + \theta_2 b$$
$$- \frac{(\kappa + k_1)(\theta_2\kappa + k_1)}{(a + b)^2}[(bt + 1)(a + b) + b]\Big]$$

$$C_2 = \frac{v^2}{2b^3}(\kappa + k_1)(\theta_2\kappa + k_1)\Big[\frac{2b - a}{(b - a)^2} + \frac{a + 2b}{(a + b)^2}\Big]$$

$$A(t) = A_2(t) - 2A_1C_1 - A_1^2 \exp[(b - a)t]$$

$$B(t) = B_2(t) - 2B_1C_1 - B_1^2 \exp[-(a + b)t]$$

$$C(t) = C_2 - C_1^2 - 2A_1B_1 \exp[-2at]$$

occur only if scour exposes buried grains to the flow (cf., Martin et al., 2014; Nakagawa & Tsujimoto, 1980; Voepel, Schumer, & Hassan, 2013). Using this terminology, we summarize when $k_2 \gg k_1 \gg \kappa$ and $\theta_1 = 1$, the variance in equation (15) expresses four scaling ranges: local, intermediate, and global, and geomorphic. We emphasize only the first three of these ranges are diffusive.

4 Discussion

The model we've presented involves four parameters. These are the characteristic velocity v of moving sediment and three key timescales: $1/k_2$, $1/k_1$, and $1/\kappa$. The timescales represent the mean duration of motion, the mean duration of rest, and the mean duration of rest before burial occurs. As shown in figure 2, scaling laws $\sigma_x^2 \propto t^\gamma$ approximately characterize the diffusion in each scaling range. The exponents γ in each range result from competition between different terms in equation (15). Between these ranges, there are crossover regions where the scaling is not a simple power law. Because these crossover regions are relatively narrow, we can approximately characterize them with crossover times T_L, T_I, and T_G. These times partition the diffusion ranges into $0 < t < T_L$ (lo-
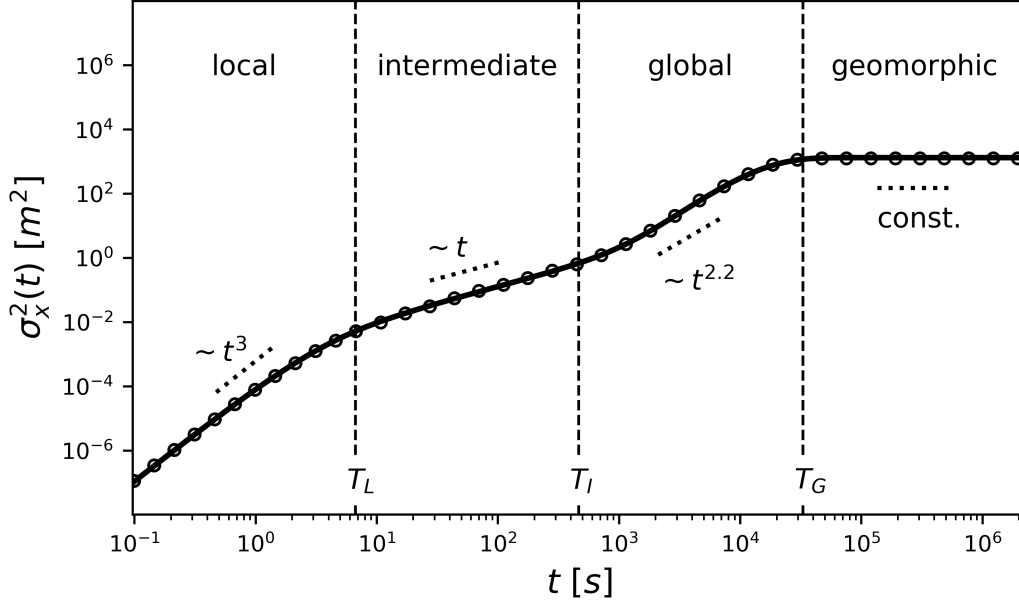
Figure 2. The variance equation (15) is plotted for the parameters $1/k_2 = 1.5$s, $1/k_1 = 30.0$s, and $v = 0.1$m/s. These values are comparable to laboratory flume experiments transporting small ($\sim$ 5mm) gravels (cf., Lajeunesse et al., 2010; Martin et al., 2012). The timescale of burial is set to $1/\kappa = 7200.0$s (two hours), and the initial condition is rest ($\theta_1 = 1$). The solid line is equation (15) while the points are directly simulated. When $k_2 \gg k_1 \gg \kappa$, as as is the case in this plot, there are four distinct scaling ranges of σ_x^2: local, intermediate, global, and geomorphic. Within each range, a slope key is added to demonstrate the scaling $\sigma_x^2 \propto t^\gamma$. There are three crossovers between these ranges, denoted on the figure by vertical lines. Crossover times T_L, T_I, and T_G are indicated at the bottom of the plot. They are given in equations (16-18) in terms of the model's input parameters.

cal), $T_L < t < T_I$ (intermediate), $T_I < t < T_G$ (global), and $T_G < t$ (geomorphic). Figure 2 depicts these crossover times as vertical lines. To understand the scale dependence expressed by the bedload variance in equation (15), we need to determine the exponents γ of each range and relate the crossover times T_L, T_I, and T_G between diffusion ranges to the model parameters v, k_1, k_2, and κ.

We determine the diffusion exponents γ in the local, intermediate, and global ranges using two limiting cases of equation (15): (1) $t \ll 1/\kappa$, and (2) $1/k_2 \to 0$ while $vk_2 =$ const. Limit (1) corresponds to times so short a negligible amount of sediment burial has occurred, while limit (2) corresponds to times so long a motion interval appears as an

instantaneous step having mean step length $l = vk_2$. We evaluate these limits in appendix C and obtain the diffusion exponents. Local range diffusion has exponent $2 \leq \gamma \leq 3$ depending on the initial conditions θ_1 and θ_2. When the initial conditions are pure, meaning one of the θ_i is zero, the local exponent is $\gamma = 3$. When grains start in a mixture of motion and rest states, meaning neither θ_i is zero, the local exponent is $\gamma = 2$. Intermediate range diffusion always has exponent $\gamma = 1$, agreeing with classic flume experiments (e.g., H. A. Einstein, 1937; Nakagawa & Tsujimoto, 1976; Yano, Tsuchiya, & Michiue, 1969). Finally, global range diffusion has exponent $1 < \gamma < 3$ depending on the ratio k_1/κ. In the extreme case $k_1/\kappa \approx 0$, we find normal diffusion $\sigma_x^2 \propto t$. However, in the opposite extreme $k_1/\kappa \to \infty$, we find super-diffusion $\sigma_x^2 \propto t^3$. For general ratios κ/k_1, the global exponent lies between these extremes. For example, when $k_1/\kappa \approx 240$ as in figure 2, the global range exponent is $\gamma \approx 2.2$. We surmise when the model parameters satisfy $k_2 \gg k_1 \gg \kappa$ meaning all three diffusion ranges exist, the variance (15) implies local range super-diffusion with exponent depending on the θ_i, intermediate range normal diffusion with no dependence on model parameters, and global range super-diffusion with exponent depending on the ratio k_1/κ. Finally, the model supports a geomorphic range of no diffusion ($\gamma = 0$) associated with the eventual and long term burial of all sediment grains.

Each of the three crossover times relates to a physical process affecting a population of grains. Exchange between motion and rest states induces the local/intermediate crossover, the onset of sediment burial induces the intermediate/global crossover, and the completion of sediment burial induces the global/geomorphic crossover. Each process admits two characteristic times, and we formulate the crossover times heuristically as geometric averages of these characteristic times:

$$T_L = \sqrt{\frac{1}{k_1}\frac{1}{k_2}}, \tag{16}$$

$$T_I = \sqrt{\frac{1}{k_1}\frac{1}{\kappa}}, \tag{17}$$

$$T_G = \sqrt{\frac{1}{\kappa}\frac{k_1 + k_2}{\kappa k_1}}. \tag{18}$$

Figure 2 depicts these relationships as dashed vertical lines. The times $1/k_1$ and $1/k_2$ characterize exchanges between motion and rest, while $1/k_1$ and $1/\kappa$ characterize the onset of burial originating from grains buried in their first resting sojourns. Equations (16) and (17) mix these paired times. The completion of sediment burial and its characteristic timescales originate from the last grains to bury. In one extreme, all grains rest on

273 the surface, meaning the last grains bury around $1/\kappa$; while in another, a fraction of grains

274 remains in motion for a long time evading burial. By analogy to the mobile-immobile

275 model of Ancey, Böhm, Jodeau, and Frey (2006), we reason that a fraction $k_1/(k_1+k_2)$

276 of the free population will be in motion and evading burial at long timescales, and for

277 this fraction we propose an effective trapping rate $\kappa k_1/(k_1+k_2)$. Equation (18) mixes

278 the reciprocal of this effective rate with $1/\kappa$. We tested formulas (16-18) for many pa-

279 rameter choices and conclude they adequately represent the crossover locations between

280 diffusion regimes provided the parameters satisfy $k_2 \gg k_1 \gg \kappa$ and grains start from

281 rest ($\theta_1 = 1$). However, starting grains from motion ($\theta_2 = 1$) widens the crossover re-

282 gion between local and intermediate ranges, meaning equation (16) loses representative

283 power; while setting relatively very large values of k_2 widens the crossover region between

284 global and geomorphic ranges, meaning equation (18) loses representative power. Ulti-

285 mately, we emphasize the representation of finite width crossover regions by crossover

286 times is an idealization, so we propose equations (16-18) as heuristics. These relations

287 provide useful divisions between the bedload diffusion scaling ranges.

288 Our four range bedload diffusion model reduces to earlier works through the two

289 simplified limits previously leveraged to extract the scaling exponents γ and explored

290 in appendix C. Limit (1) implies the model developed by Lisle et al. (1998) to describe

291 soil transport within a sheet flow, while limit (2) implies the model developed by Wu et

292 al. (2019) to describe bedload transport with burial. Either of these cases further sim-

293 plifies to the classic results of H. A. Einstein (1937) and his early followers (e.g., Hubbell

294 & Sayre, 1964; Nakagawa & Tsujimoto, 1976; Yano, 1969) that predict a single range

295 of normal diffusion. Lisle et al. (1998) generalized the Einstein model to include a finite

296 velocity and duration of motion in place of instantaneous steps, and they derived two

297 ranges of diffusion – super-diffusive and normal. Wu et al. (2019) developed an active

298 layer formulation of bedload transport where grains are transferred from the active layer

299 (surface) to the substrate layer (burial) at a constant rate. They simplified the problem

300 by interpreting motions as instantaneous steps, and they derived two ranges of diffusion

301 – normal and super-diffusive. Our model ultimately extends these two works and re-frames

302 them in the formalism of CTRWs (e.g., Weiss, 1994) that was implicitly applied by H. A. Ein-

303 stein (1937).

304 We offer several implications of our model for bedload diffusion studies in gravel

305 bed streams. First, our model confines the valid range of scale independent models such

as the advection-diffusion equation (e.g., D. N. Bradley, Tucker, & Benson, 2010) and the Einstein model (e.g., Martin et al., 2012) for practical applications such as contaminant transport (e.g Macklin et al., 2006; Malmon, Reneau, Dunne, Katzman, & Drakos, 2005) and aquatic habitat restoration (e.g., Gaeuman, Stewart, Schmandt, & Pryor, 2017). We can conclude when the observation timescale satisfies $T_L < t < T_I$, with T_L and T_I given by equations (16) and (17), we expect normal bedload diffusion $\sigma_x^2 = D_d t$. Second, the model links bedload transport understanding across scales. In practice, we might measure sediment diffusion within a channel on one timescale with intent to apply our knowledge at smaller or larger timescales; usually, experimental limitations constrain the measurement timescale. For example, we could determine k_1 and k_2 by measuring the virtual velocity and diffusivity of sediment tracers in the intermediate range (e.g., H. A. Einstein, 1937; Nakagawa & Tsujimoto, 1976; Yano et al., 1969). With an estimate of the trapping rate κ, equation (15) provides diffusion characteristics of the global range $T_I < t < T_G$ which is more difficult to study experimentally.

To describe the scale dependence of bedload diffusion, we extended the original Einstein model by building up ideas from condensed matter physics. Along the way, we incorporated two simplifying assumptions that deserve further research attention. First, we treated sediment burial as a quasi permanent condition; and second, we implicitly assumed burial is the only process trapping grains in river channels. In actuality, burial is a temporary condition linked to scour and fill of the sedimentary bed (Hassan & Church, 1994; Martin et al., 2014; Voepel et al., 2013), and field experiments show other processes trapping sediment. For example, grains can become stranded on bars (N. D. Bradley, 2017; Ferguson & Hoey, 2002) and embedded in stabilizing structures such as steps or clusters (e.g. Church, Hassan, & Wolcott, 1998; Hassan et al., 2008). In principle, the multi state CTRW framework we developed here can describe bedload diffusion with multiple trapping processes by simply adding more states, and it can handle impermanent sojourns in these states by specifying propagators for them. Unfortunately, we currently lack the experimental knowledge to specify these propagators, since trapping rates and durations are poorly understood in association with particular processes. For example, recent experiments have attributed resting times to any immobile sediment, and this is known to imply heavy-tailed sediment resting time distributions (e.g., N. D. Bradley, 2017; Olinde & Johnson, 2015). However, very few studies have resolved immobile times of sediment while identifying their underlying mechanism (e.g., Martin et al., 2014). We

propose experiments to determine the rates and durations of specific bedload trapping

processes as important topics for further study. A first step might be to measure the burial

rate κ we applied in this paper; in principle, this could be discerned by timing the pe-

riod required for tagged surface grains to become buried in flume experiments. Once bet-

ter understanding of the rates and durations of sediment trapping processes is in place,

generalizations built from the framework we've presented in this paper should better pre-

dict bedload diffusion on the global and geomorphic scales.

5 Conclusion

We developed a random walk model with alternating mobile and immobile states

and a possibility of trapping from the immobile state, and we used it to describe sed-

iment transporting through a river channel as it gradually becomes buried. To our knowl-

edge, this is the first analytical description of bedload diffusion across the local, inter-

mediate, and global timescales introduced by Nikora et al. (2001). Pushing the ideas of

Nikora et al. somewhat further, we proposed a geomorphic range to describe diffusion

characteristics at timescales larger than the global range. At base level, our model demon-

strates the required components for three bedload diffusion ranges: (1) the duration of

sediment motions, (2) mobile-immobile switching, and (3) a sediment trapping process.

A next step is to incorporate the bed scour process that re-exposes buried sediment to

better understand the global and geomorphic ranges. Ultimately, we emphasize the multi

state random walk formalism used in this paper implicitly underlies most existing bed-

load diffusion models, and we believe it will readily accommodate efforts to include more

physical processes into Einstein's research paradigm.

A Calculation of the distribution function

Double transforming (1-3) using the definition (10) gives

$$\tilde{\omega}_{1T}(\eta, s) = \theta_1 \tilde{g}_1(\eta, s) + \tilde{\omega}_2(\eta, s)\tilde{g}_1(\eta, s) - \tilde{\omega}_{1F}(\eta, s), \tag{A.1}$$

$$\tilde{\omega}_{1F}(\eta, s) = \theta_1 \tilde{g}_1(\eta, s + \kappa) + \tilde{\omega}_2(\eta, s)\tilde{g}_1(\eta, s + \kappa), \tag{A.2}$$

$$\tilde{\omega}_2(\eta, s) \quad = \theta_2 \tilde{g}_2(\eta, s) + \tilde{\omega}_{1F}(\eta, s)\tilde{g}_2(\eta, s). \tag{A.3}$$

This algebraic system solves for

$$\tilde{\omega}_{1T}(\eta, s) = \frac{\theta_1 + \theta_2 \tilde{g}_2(\eta, s)}{1 - \tilde{g}_1(\eta, s + \kappa)\tilde{g}_2(\eta, s)} \big\{ \tilde{g}_1(\eta, s) - \tilde{g}_1(\eta, s + \kappa) \big\}, \tag{A.4}$$

$$\tilde{\omega}_{1F}(\eta, s) = \frac{\theta_1 + \theta_2 \tilde{g}_2(\eta, s)}{1 - \tilde{g}_1(\eta, s + \kappa)\tilde{g}_2(\eta, s)} \tilde{g}_1(\eta, s + \kappa), \tag{A.5}$$

$$\tilde{\omega}_2(\eta, s) = \frac{\theta_2 + \theta_1 \tilde{g}_1(\eta, s + \kappa)}{1 - \tilde{g}_1(\eta, s + \kappa)\tilde{g}_2(\eta, s)} \tilde{g}_2(\eta, s). \tag{A.6}$$

Double transforming (4-6) gives

$$\tilde{p}_0(\eta, s) = \frac{1}{s} \tilde{\omega}_{1T}(\eta, s), \tag{A.7}$$

$$\tilde{p}_1(\eta, s) = \theta_1 \tilde{G}_1(\eta, s) + \tilde{\omega}_2(\eta, s)\tilde{G}_1(\eta, s), \tag{A.8}$$

$$\tilde{p}_2(\eta, s) = \theta_2 \tilde{G}_2(\eta, s) + \tilde{\omega}_{1F}(\eta, s)\tilde{G}_2(\eta, s). \tag{A.9}$$

The total probability is $p(x,t) = p_0(x,t) + p_1(x,t) + p_2(x,t)$. Using equations (A.4-A.9) this becomes, in the double Laplace representation,

$$\tilde{p}(\eta, s) = \frac{1}{s} \frac{\theta_1 + \theta_2 \tilde{g}_2(\eta, s)}{1 - \tilde{g}_1(\eta, s + \kappa)\tilde{g}_2(\eta, s)} \big\{ \tilde{g}_1(\eta, s) - \tilde{g}_1(\eta, s + \kappa) \big\}$$
$$+ \frac{\theta_1 \big[\tilde{G}_1(\eta, s) + \tilde{g}_1(\eta, s + \kappa)\tilde{G}_2(\eta, s) \big] + \theta_2 \big[\tilde{G}_2(\eta, s) + \tilde{g}_2(\eta, s)\tilde{G}_1(\eta, s) \big]}{1 - \tilde{g}_1(\eta, s + \kappa)\tilde{g}_2(\eta, s)}. \tag{A.10}$$

Plugging the propagators outlined in equations (8-9) into equation (A.10) gives

$$\tilde{p}(\eta, s) = \frac{1}{s} \frac{(s + \kappa + k')s + \theta_1(s + \kappa)\eta v + \kappa k_2}{(s + \kappa + k_1)\eta v + (s + \kappa + k')s + \kappa k_2}. \tag{A.11}$$

In this equation, $k' = k_1 + k_2$, and we have used the normalization requirement of the initial probabilities: $\theta_1 + \theta_2 = 1$. The double inverse transform of this equation provides the distribution $p(x,t)$. We invert the transform over η first. Using the results 15.103 (transform of exponential), 15.123 (transform of derivative), and 15.141 (transform of Dirac delta function) from Arfken (1985) provides

$$\tilde{p}(x, s) = \theta_1 \frac{s + \kappa}{s(s + \kappa + k_1)} \delta(x) + \frac{1}{v} \bigg(\frac{(s + \kappa + k')s + \kappa k_2}{s(s + \kappa + k_1)}$$
$$- \frac{\theta_1(s + \kappa)[s(s + \kappa + k_1) + \kappa k_2]}{s(s + \kappa + k_1)^2} \bigg) \exp\bigg[- \frac{(s + \kappa + k')s + \kappa k_2}{s + \kappa + k_1} \frac{x}{v} \bigg]. \tag{A.12}$$

Inverting the remaining transform over s, applying results 15.152 (substitution), 15.164 (translation), and 15.175 (transform of te^{kt}) from Arfken (1985), and defining the shorthand notations $\tau = k_1(t - x/v)$, $\xi = k_2 x/v$, and $\Omega = (\kappa + k_1)/k_1$, gives the simpler

form

$$
\begin{aligned}
p(x,t) = \theta_1 \Big[1 - &\frac{k_1}{\kappa + k_1} \big(1 - e^{-(\kappa + k_1)t} \big) \Big] \delta(x) + \frac{1}{v} \exp[\Omega\tau - \xi] \\
&\times \mathcal{L}^{-1} \Big\{ \Big(\theta_2 + \frac{\theta_1 k_1 + \theta_2 k_2}{s} + \frac{\theta_1 k_1 k_2}{s^2} + \frac{\theta_2 \kappa k_2}{s(s - \kappa - k_1)} + \frac{\theta_1 \kappa k_1 k_2}{s^2(s - \kappa - k_1)} \Big) \\
&\hspace{8cm} \times \exp\Big[\frac{k_1 \xi}{s} \Big]; \tau/k_1 \Big\}. \quad \text{(A.13)}
\end{aligned}
$$

Using entries 2.2.2.1, 2.2.2.8, and 1.1.1.13 from Prudnikov, Brychkov, and Marichev (1992) in conjunction with the definition of the Marcum Q-function $\mathcal{P}_\mu(x,t)$ (e.g., Temme, 1996), and inserting the Heaviside functions to account for the fact that grains can neither travel backwards nor at speeds exceeding v, we finally arrive at equation (12) for the joint distribution $p(x,t)$.

B Calculation of the moments

We compute the first two moments of position x and ultimately its variance using equation (11). The first two derivatives of the double Laplace transformed distribution (A.11) are

$$
\partial_\eta \tilde{p}(\eta, s) = -v \frac{1}{s} \frac{[(s + \kappa + k')s + \kappa k_2][\theta_2(s + \kappa) + k_1]}{[\eta v(s + \kappa + k_1) + (s + \kappa + k')s + \kappa k_2]^2}, \quad \text{(B.1)}
$$

$$
\partial_\eta^2 \tilde{p}(\eta, s) = 2v^2 \frac{1}{s} \frac{(s + \kappa + k_1)[(s + \kappa + k')s + \kappa k_2][\theta_2(s + \kappa) + k_1]}{[\eta v(s + \kappa + k_1) + (s + \kappa + k')s + \kappa k_2]^3}. \quad \text{(B.2)}
$$

Evaluating these at $\eta = 0$ and applying equation (11) provides the Laplace transformed moments

$$
\frac{\langle \tilde{x}(s) \rangle}{v} = \frac{1}{s} \frac{\theta_2(s + \kappa) + k_1}{(s + \kappa + k')s + \kappa k_2} = \frac{1}{s} \frac{\theta_2(s + \kappa) + k_1}{(s + a + b)(s + a - b)}, \quad \text{(B.3)}
$$

$$
\frac{\langle \tilde{x}^2(s) \rangle}{2v^2} = \frac{1}{s} \frac{(s + \kappa + k_1)(\theta_2(s + \kappa) + k_1)}{[(s + \kappa + k')s + \kappa k_2]^2} = \frac{1}{s} \frac{(s + \kappa + k_1)(\theta_2(s + \kappa) + k_1)}{(s + a + b)^2(s + a - b)^2}. \quad \text{(B.4)}
$$

The parameters $a = (\kappa + k')/2$ and $b^2 = a^2 - \kappa k_2$ were introduced to factorize the denominators. These equations can be inverted using the properties 15.164 (translation), 15.11.1 (integration), and 15.123 (differentiation) from Arfken (1985) after expansion in partial fractions. For the mean, the calculation is

$$
\frac{2b}{v} \langle x \rangle = \Big[\theta_2 + (k_1 + \theta_2 \kappa) \int_0^t dt \Big] \mathcal{L}^{-1} \Big\{ \frac{1}{s + a - b} - \frac{1}{s + a + b}; t \Big\} \quad \text{(B.5)}
$$

$$
= \Big[\theta_2 + \frac{k_1 + \theta_2 \kappa}{b - a} \Big] e^{(b-a)t} - \Big[\theta_2 - \frac{k_1 + \theta_2 \kappa}{a + b} \Big] e^{-(a+b)t} - \Big[\frac{k_1 + \theta_2 \kappa}{b - a} + \frac{k_1 + \theta_2 \kappa}{a + b} \Big]. \quad \text{(B.6)}
$$

This equation rearranges to (13). The second moment (B.4) is

$$
\frac{2b^2}{v^2}\langle x^2\rangle = \left[\theta_2(\delta(t)+\partial_t) + (\theta_2(2\kappa+k_1)+k_1) + (\kappa+k_1)(\theta_2\kappa+k_1)\int_0^t dt\right]
$$
$$
\times \mathcal{L}^{-1}\left\{\frac{1}{(s+a-b)^2} + \frac{1}{(s+a+b)^2} - \frac{1}{b(s+a-b)} + \frac{1}{b(s+a+b)};t\right\}. \quad \text{(B.7)}
$$

This becomes

$$
\frac{2b^3}{v^2}\langle x^2\rangle = \left[\theta_2\partial_t + [\theta_2(2\kappa+k_1)+k_1] + (\kappa+k_1)(\theta_2\kappa+k_1)\int_0^t dt\right]
$$
$$
\times \left((bt-1)e^{(b-a)t} + (bt+1)e^{-(a+b)t}\right) \quad \text{(B.8)}
$$

which evaluates to equation (14). $\sigma_x^2 = \langle x^2\rangle - \langle x\rangle^2$ derives the variance in equation (15).

C Limiting behavior of the moments

Limit (1) is $\kappa \to 0$. We take this limit in equations (B.3) and (B.4) with initial condition $\theta_1 = 1$ to obtain

$$
\langle\tilde{x}\rangle = vk_1\frac{1}{s^2(s+k')}, \quad \text{(C.1)}
$$

$$
\langle\tilde{x}^2\rangle = 2v^2k_1\frac{s+k_1}{s^3(s+k')^2}. \quad \text{(C.2)}
$$

Inverting these equations provides the variance

$$
\sigma_x^2 = 2v^2\frac{k_1}{k'^4}\left(k_1\Big[\frac{1}{2} - k'te^{-k't} - \frac{1}{2}e^{-2k't}\Big] + k_2\Big[-2+k't+(2+k't)e^{-k't}\Big]\right). \quad \text{(C.3)}
$$

This result encodes two ranges of diffusion and can also be derived from the governing equations of the Lisle et al. (1998) model. Expanding for small t provides $\sigma_x^2(t) = v^2k_1t^3/3$ – local range super-diffusion. Expanding for large t provides $\sigma_x^2(t) = 2v^2k_1k_2t/k'^3$ – intermediate range normal diffusion.

We further investigate limit (1) for arbitrary initial conditions. By applying Tauberian theorems, we assert the $t \to 0$ variance is determined by the $s \to \infty$ limits of (B.3) and (B.4) (e.g., Weeks & Swinney, 1998; Weiss, 1994). Expanding these equations in powers of $1/s$ and inverting the resulting transforms gives

$$
\langle x\rangle = v\theta_2 t + \frac{1}{2}v(\theta_1 k_1 - \theta_2 k_2)t^2 + O(t^3), \quad \text{(C.4)}
$$

$$
\langle x^2\rangle = v^2\theta_2 t^2 + \frac{1}{3}v^2(\theta_1 k_1 - 2\theta_2 k_2)t^3 + O(t^4). \quad \text{(C.5)}
$$

This equation highlights the effect of initial conditions on the diffusion characteristics of the local range:

$$
\sigma_x^2(t) \sim v^2\theta_1\theta_2 t^2 + \frac{1}{3}v^2(\theta_1 k_1 + \theta_2 k_2)t^3. \quad \text{(C.6)}
$$

We have taken only leading order terms for any option of θ_1 and θ_2. Equation (C.6) shows local range exponent $\gamma = 2$ when initial conditions are mixed (both are non-zero) and $\gamma = 3$ when initial conditions are pure (one is zero).

Limit (2) is $1/k_2 \to 0$ and $v \to \infty$ while $v/k_2 = l$. Under this limit, equations (B.3) and (B.4) provide

$$\langle \tilde{x} \rangle = k_1 l \frac{1}{s(s+\kappa)}, \tag{C.7}$$

$$\langle \tilde{x}^2 \rangle = 2l^2 k_1 \frac{s + \kappa + k_1}{s(s+\kappa)^2}. \tag{C.8}$$

Inverting these equations and introducing the variables $c = lk_1$ (an effective velocity) and $D_d = l^2 k_1$ (a diffusivity) provides positional variance

$$\sigma_x^2(t) = \frac{2D_d(1 - e^{-\kappa t})}{\kappa} + \frac{(1 - e^{-2\kappa t} - 2e^{-\kappa t}\kappa t)c^2}{\kappa^2}. \tag{C.9}$$

This is mathematically identical to the key result of Wu et al. (2019). Expanding for small t provides $\sigma_x^2(t) = 2D_d t$ – intermediate range normal diffusion, while sending $t \to \infty$ provides $\sigma_x^2 = (2D_d\kappa + c^2)/\kappa^2$ – a constant variance in the geomorphic range. The global range is characterized by competition between terms in equation (C.9), and shows $2 \leq \gamma \leq 3$ depending on the ratio k_1/κ (cf., Wu et al., 2019). Finally, both equations (C.3) and (C.9) reduce to the Einstein result $\sigma_x^2(t) = 2D_d t$ in further simplified limits.

Acknowledgments

References

Ancey, C., Böhm, T., Jodeau, M., & Frey, P. (2006). Statistical description of sediment transport experiments. *Physical Review E - Statistical, Nonlinear, and Soft Matter Physics*, *74*(1), 1–14. doi: 10.1103/PhysRevE.74.011302

Arfken, G. (1985). *Mathematical Methods for Physicists*. Academic Press, Inc. doi: 10.1063/1.3062258

Barik, D., Ghosh, P. K., & Ray, D. S. (2006). Langevin dynamics with dichotomous noise; Direct simulation and applications. *Journal of Statistical Mechanics: Theory and Experiment*(3). doi: 10.1088/1742-5468/2006/03/P03010

Berezhkovskii, A. M., & Weiss, G. H. (2002). Detailed description of a two-state non-Markov system. *Physica A: Statistical Mechanics and its Applications*, *303*(1-2), 1–12. doi: 10.1016/S0378-4371(01)00431-9

Berkowitz, B., Cortis, A., Dentz, M., & Scher, H. (2006). Modeling Non-fickian transport in geological formations as a continuous time random walk. *Reviews of Geophysics*, *44*(2), 1–49. doi: 10.1029/2005RG000178

Bialik, R. J., Nikora, V. I., & Rowiński, P. M. (2012). 3D Lagrangian modelling of saltating particles diffusion in turbulent water flow. *Acta Geophysica*, *60*(6), 1639–1660. doi: 10.2478/s11600-012-0003-2

Bradley, D. N., Tucker, G. E., & Benson, D. A. (2010). Fractional dispersion in a sand bed river. *Journal of Geophysical Research*, *115*, F00A09. Retrieved from http://doi.wiley.com/10.1029/2009JF001268 doi: 10.1029/2009JF001268

Bradley, N. D. (2017). Direct Observation of Heavy-Tailed Storage Times of Bed Load Tracer Particles Causing Anomalous Superdiffusion. *Geophysical Research Letters*, *44*(24), 12,227–12,235. doi: 10.1002/2017GL075045

Church, M., Hassan, M. a. M. M. A., & Wolcott, J. F. J. (1998). Stabilizing self-organized structures in gravel-bed stream channels: Field and experimental observations. *Water Resources Research*, *34*(11), 3169. doi: 10.1029/98WR00484

Daly, E., & Porporato, A. (2010). Effect of different jump distributions on the dynamics of jump processes. *Physical Review E - Statistical, Nonlinear, and Soft Matter Physics*, *81*(6), 1–10. doi: 10.1103/PhysRevE.81.061133

Einstein, A. (1905). Brownian Movement. *Biotropica*, *1*. doi: 10.5167/uzh-53657

Einstein, H. A. (1937). *Bed-load transport as a probability problem* (Unpublished doctoral dissertation). ETH Zurich.

Ettema, R., & Mutel, C. F. (2004). Hans Albert Einstein: Innovation and Compromise in Formulating Sediment Transport by Rivers. *Journal of Hydraulic Engineering*, *130*(6), 477–487. doi: 10.1061/(ASCE)0733-9429(2004)130:6(477)

Fan, N., Singh, A., Guala, M., Foufoula-Georgiou, E., & Wu, B. (2016). Exploring

470 a semimechanistic episodic Langevin model for bed load transport: Emergence
471 of normal and anomalous advection and diffusion regimes. *Water Resources*
472 *Research*, *52*(4), 3787–3814. doi: 10.1002/2016WR018704.Received

473 Ferguson, R. I., & Hoey, T. B. (2002). Long-term slowdown of river tracer pebbles:
474 Generic models and implications for interpreting short-term tracer studies.
475 *Water Resources Research*, *38*(8), 17–1–17–11. doi: 10.1029/2001wr000637

476 Gaeuman, D., Stewart, R., Schmandt, B., & Pryor, C. (2017). Geomorphic re-
477 sponse to gravel augmentation and high-flow dam release in the Trinity River,
478 California. *Earth Surface Processes and Landforms*, *42*(15), 2523–2540. doi:
479 10.1002/esp.4191

480 Ganti, V., Meerschaert, M. M., Foufoula-Georgiou, E., Viparelli, E., & Parker, G.
481 (2010). Normal and anomalous diffusion of gravel tracer particles in rivers.
482 *Journal of Geophysical Research: Earth Surface*, *115*. Retrieved from `http://`
483 `doi.wiley.com/10.1029/2008JF001222` doi: 10.1029/2008JF001222

484 Giddings, J. C., & Eyring, H. (1955). A molecular dynamic theory of chromatogra-
485 phy. *Journal of Physical Chemistry*, *59*(5), 416–420.

486 Gordon, R., Carmichael, J. B., & Isackson, F. J. (1972). Saltation of Plastic Balls in
487 a 'One-Dimensional' Flume. *Water Resources Research*, *8*(2), 444–458. doi: 10
488 .1029/WR008i002p00444

489 Hassan, M. A., & Church, M. (1994). Vertical mixing of coarse particles in gravel
490 bed rivers: A kinematic model. *Water Resources Research*, *30*(4), 1173–1185.
491 doi: 10.1029/93WR03351

492 Hassan, M. A., Church, M., & Schick, A. P. (1991). Distance of movement of coarse
493 particles in gravel bed streams. *Water Resources Research*, *27*(4), 503–511.
494 doi: 10.1029/90WR02762

495 Hassan, M. A., Smith, B. J., Hogan, D. L., Luzi, D. S., Zimmermann, A. E., &
496 Eaton, B. C. (2008). Sediment storage and transport in coarse bed streams:
497 scale considerations. In H. Habersack & H. Piegay (Eds.), *Gravel-bed rivers*
498 *8: From process understanding to river restoration* (Vol. 11, pp. 473–496).
499 Elsevier B.V. doi: 10.1016/S0928-2025(07)11137-8

500 Hubbell, D. W., & Sayre, W. W. (1964). Sand Transport Studies with Radioactive
501 Tracers. *J. Hydr. Div.*, *90*(HY3), 39–68.

502 Jeon, J. H., Monne, H. M. S., Javanainen, M., & Metzler, R. (2012). Anomalous dif-

fusion of phospholipids and cholesterols in a lipid bilayer and its origins. *Physical Review Letters*, *109*(18), 1–5. doi: 10.1103/PhysRevLett.109.188103

Kittel, C. (1958). *Elementary Statistical Physics*. R.E. Krieger Pub. Co.

Lajeunesse, E., Malverti, L., & Charru, F. (2010). Bed load transport in turbulent flow at the grain scale: Experiments and modeling. *Journal of Geophysical Research: Earth Surface*, *115*(4). doi: 10.1029/2009JF001628

Lisle, I. G., Rose, C. W., Hogarth, W. L., Hairsine, P. B., Sander, G. C., & Parlange, J.-Y. (1998). Stochastic sediment transport in soil erosion. *Journal of Hydrology*, *204*, 217–230.

Macklin, M. G., Brewer, P. A., Hudson-Edwards, K. A., Bird, G., Coulthard, T. J., Dennis, I. A., ... Turner, J. N. (2006). A geomorphological approach to the management of rivers contaminated by metal mining. *Geomorphology*, *79*(3-4), 423–447. doi: 10.1016/j.geomorph.2006.06.024

Malmon, D. V., Dunne, T., & Reneau, S. L. (2003). Stochastic Theory of Particle Trajectories through Alluvial Valley Floors. *The Journal of Geology*, *111*(5), 525–542. doi: 10.1086/376764

Malmon, D. V., Reneau, S. L., Dunne, T., Katzman, D., & Drakos, P. G. (2005). Influence of sediment storage on downstream delivery of contaminated sediment. *Water Resources Research*, *41*(5), 1–17. doi: 10.1029/2004WR003288

Marcum, J. (1960). A statistical theory of target detection by pulse radar. *IRE Trans. Inform. Theory*, *6*, 59–268.

Martin, R. L., Jerolmack, D. J., & Schumer, R. (2012). The physical basis for anomalous diffusion in bed load transport. *Journal of Geophysical Research: Earth Surface*, *117*(1), 1–18. doi: 10.1029/2011JF002075

Martin, R. L., Purohit, P. K., & Jerolmack, D. J. (2014). Sedimentary bed evolution as a mean-reverting random walk: Implications for tracer statistics. *Geophysical Research Letters*, *41*(17), 6152–6159. doi: 10.1002/2014GL060525

Metzler, R., & Klafter, J. (2000). The random walk's guide to anomalous diffusion: A fractional dynamics approach. *Physics Report*, *339*(1), 1–77. doi: 10.1016/S0370-1573(00)00070-3

Molina-Garcia, D., Sandev, T., Safdari, H., Pagnini, G., Chechkin, A., & Metzler, R. (2018). Crossover from anomalous to normal diffusion: Truncated power-law noise correlations and applications to dynamics in lipid bilayers. *New Journal*

of Physics, *20*(10). doi: 10.1088/1367-2630/aae4b2

Montroll, E. W., & Weiss, G. H. (1965). Random Walks on Lattices. II. *Journal of Mathematical Physics*, *6*, 167–181.

Nakagawa, H., & Tsujimoto, T. (1976). On Probabilistic Characteristics of Motion of Individual Sediment Particles on Stream Beds. In *Hydraulic problems solved by stochastic methods: Second international iahr symposium on stochastic hydraulics* (pp. 293–320). Lund, Sweden.

Nakagawa, H., & Tsujimoto, T. (1980). Sand bed instability due to bed load motion. *Journal of the Hydraulics Division-ASCE*.

Nikora, V., Habersack, H., Huber, T., & McEwan, I. (2002). On bed particle diffusion in gravel bed flows under weak bed load transport. *Water Resources Research*, *38*(6), 1–9. Retrieved from http://doi.wiley.com/10.1029/2001WR000513 doi: 10.1029/2001WR000513

Nikora, V., Heald, J., Goring, D., & McEwan, I. (2001). Diffusion of saltating particles in unidirectional water flow over a rough granular bed. *Journal of Physics A: Mathematical and General*, *34*(50). doi: 10.1088/0305-4470/34/50/103

Olinde, L., & Johnson, J. P. L. (2015). Using RFID and accelerometer-embedded tracers to measure probabilities of bed load transport, step lengths, and rest times in a mountain stream. *Water Resources Research*, *51*, 7572–7589. doi: 10.1002/2014WR016259

Phillips, C. B., Martin, R. L., & Jerolmack, D. J. (2013). Impulse framework for unsteady flows reveals superdiffusive bed load transport. *Geophysical Research Letters*, *40*(7), 1328–1333. doi: 10.1002/grl.50323

Prudnikov, A., Brychkov, Y. A., & Marichev, O. (1992). *Integrals and Series: Volume 5: Inverse Laplace Transforms*. Gordon and Breach Science Publishers.

Reynolds, A., & Rhodes, C. (2009). The Levy flight paradigm: random search patterns and mechanisms. *Ecology*, *90*(4), 877–887.

Schmidt, M. G., Sagués, F., & Sokolov, I. M. (2007). Mesoscopic description of reactions for anomalous diffusion: A case study. *Journal of Physics Condensed Matter*, *19*(6). doi: 10.1088/0953-8984/19/6/065118

Sokolov, I. M. (2012). Models of anomalous diffusion in crowded environments. *Soft Matter*, *8*(35), 9043–9052. doi: 10.1039/c2sm25701g

Taylor, G. I. (1920). Diffusion by continuous movements. *Proceedings of the London*

Mathematical Society, *s2-20*(1), 196–212.

Temme, N. M. (1996). *Special functions: An introduction to the classical functions of mathematical physics.* John Wiley & Sons Ltd.

Vallaeys, V., Tyson, R. C., Lane, W. D., Deleersnijder, E., & Hanert, E. (2017). A Lévy-flight diffusion model to predict transgenic pollen dispersal. *Journal of the Royal Society Interface*, *14*(126). doi: 10.1098/rsif.2016.0889

Voepel, H., Schumer, R., & Hassan, M. A. (2013). Sediment residence time distributions: Theory and application from bed elevation measurements. *Journal of Geophysical Research: Earth Surface*, *118*(4), 2557–2567. doi: 10.1002/jgrf .20151

Weeks, E. R., & Swinney, H. L. (1998). Anomalous diffusion resulting from strongly asymmetric random walks. *Physical Review E - Statistical Physics, Plasmas, Fluids, and Related Interdisciplinary Topics*, *57*(5), 4915–4920. doi: 10.1103/ PhysRevE.57.4915

Weiss, G. H. (1976). The two-state random walk. *Journal of Statistical Physics*, *15*(2), 157–165. doi: 10.1007/BF01012035

Weiss, G. H. (1994). *Aspects and applications of the random walk.* Amsterdam: North Holland.

Wu, Z., Foufoula-Georgiou, E., Parker, G., Singh, A., Fu, X., & Wang, G. (2019). Analytical solution for anomalous diffusion of bedload tracers gradually undergoing burial. *Journal of Geophysical Research: Earth Surface*, *124*(1), 21–37. doi: 10.1029/2018JF004654

Yang, C. T., & Sayre, W. W. (1971). Stochastic model for sand dispersion. *Journal of the Hydraulics Division, ASCE*, *97*(HY2).

Yang, X. R., & Wang, Y. (2019). Ubiquity of anomalous transport in porous media: Numerical evidence, continuous time random walk modelling, and hydrodynamic interpretation. *Scientific Reports*, *9*(1), 1–11. Retrieved from http://dx.doi.org/10.1038/s41598-019-39363-3 doi: 10.1038/s41598-019-39363-3

Yano, K. (1969). Tracer Studies on the Movement of Sand and Gravel. In *Proceedings of the 12th congress iahr, vol 2.* (pp. 121–129). Kyoto, Japan.

Yano, K., Tsuchiya, Y., & Michiue, M. (1969). Studies on the Sand Transport in Streams with Tracers. *Bull. Disas. Prev. Res. Inst. Kyoto Univ.*, *18*(Part 3,

602   No. 141).

603   Zhang, Y., Meerschaert, M. M., & Packman, A. I.   (2012).   Linking fluvial bed sedi-

604   ment transport across scales.   *Geophysical Research Letters*, *39*(20), 1–6.   doi:

605   10.1029/2012GL053476